

## MAGNETAR-DRIVEN MAGNETIC TOWER AS A MODEL FOR GAMMA-RAY BURSTS AND ASYMMETRIC SUPERNOVAE

DMITRI A. UZDENSKY<sup>1</sup> & ANDREW I. MACFADYEN<sup>2</sup>(Dated: September 1, 2006)  
*Draft version December 2, 2006*

## ABSTRACT

We consider a newly-born millisecond magnetar, focusing on its interaction with the dense stellar plasma in which it is initially embedded. We argue that the confining pressure and inertia of the surrounding plasma acts to collimate the magnetar's Poynting-flux-dominated outflow into tightly beamed jets and increases its magnetic luminosity. We propose this process as an essential ingredient in the magnetar model for gamma-ray burst and asymmetric supernova central engines. We introduce the "pulsar-in-a-cavity" as an important model problem representing a magnetized rotating neutron star inside a collapsing star. We describe its essential properties and derive simple estimates for the evolution of the magnetic field and the resulting spin-down power. We find that the infalling stellar mantle confines the magnetosphere, enabling a gradual build-up of the toroidal magnetic field due to continuous twisting. The growing magnetic pressure eventually becomes dominant, resulting in a magnetically-driven explosion. The initial phase of the explosion is quasi-isotropic, potentially exposing a sufficient amount of material to  $^{56}\text{Ni}$ -producing temperatures to result in a bright supernova. However, if significant expansion of the star occurs prior to the explosion, then very little  $^{56}\text{Ni}$  is produced and no supernova is expected. In either case, hoop stress subsequently collimates the magnetically-dominated outflow, leading to the formation of a magnetic tower. After the star explodes, the decrease in bounding pressure causes the magnetic outflow to become less beamed. However, episodes of late fallback can reform the beamed outflow, which may be responsible for late X-ray flares.

*Subject headings:* gamma rays: bursts — magnetic fields — pulsars: general — stars: magnetic fields — stars: neutron — supernovae: general

## 1. INTRODUCTION

In the classical collapsar scenario for long-duration gamma-ray bursts (GRBs), the core of a rotating massive star collapses to form a black hole, whereas the overlying stellar material possesses enough angular momentum to form an accretion disk that persists for at least several seconds, long enough for its jet to breakout from the star (Woosley 1993; Paczynski 1998; MacFadyen & Woosley 1999). This accretion disk—black hole system then acts as a central engine for the GRB. The power for the explosion comes both from accretion energy, released via neutrinos and perhaps via a magnetic mechanism (e.g., the magnetic tower mechanism as proposed by Uzdensky & MacFadyen 2006), and from the black-hole rotational energy, released via the Blandford–Znajek (1977) mechanism.

In the present paper we investigate an alternative scenario, in which the central object formed as a result of core collapse is not a black hole, but rather a rapidly-rotating (millisecond) magnetar with a large-scale poloidal magnetic field of the order of  $10^{15}$  G. Such a strong magnetic field can be produced, for example, by a turbulent  $\alpha - \Omega$  dynamo driven by convection in a proto-neutron star (PNS) subject to neutrino cooling (Duncan & Thompson 1992; Thompson & Duncan 1993). An alternative possibility is that the progenitor core of about  $10^4$  km has a magnetic field of order  $10^9$  G, similar to the field levels actually observed in some white dwarf of similar size. When such a highly-magnetized core collapses into a neutron star of 10 km radius, flux freezing leads to amplification of the magnetic field to  $10^{15}$  G, as dis-

cussed in Uzdensky & MacFadyen (2006). In addition, calculations by Akiyama et al. (2003) have shown that turbulent dynamo driven by the magneto-rotational instability (MRI) in the collapsing differentially-rotating core is capable of producing  $10^{15} - 10^{16}$  G fields within about 100 km from the center, on the timescale of just a few tens of milliseconds after the bounce. Whatever the origin of the very strong magnetic field in the PNS is, in this paper we shall take it for granted. Our main goal will be to investigate the role such a strong field plays in the explosion dynamics.

The idea of using a millisecond magnetar as a central engine for gamma-ray bursts has been first proposed by Usov (1992) in the context of accretion-induced collapse of a highly-magnetic ( $10^9$  G) white dwarf and, independently, by Duncan & Thompson (1992). It has been further developed and applied to different explosion scenarios by several authors (e.g., Thompson 1994; Yi & Blackman 1998; Nakamura 1998; Spruit 1999; Wheeler et al. 2000, 2002; Ruderman et al. 2000; Lyutikov & Blandford 2002; Thompson et al. 2004). The present paper is also devoted to investigating the millisecond-magnetar scenario, but viewed within the overall context of a collapsing star.

At the most basic level, the main idea is that a GRB (or a supernova) explosion is powered by the magnetic extraction of rotational energy of the newly-born rapidly-rotating magnetar. This magnetic luminosity operates alongside the much stronger neutrino cooling, which is the main avenue for releasing the gravitational binding energy of the young, still-contracting neutron star. However, most of the neutrinos escape to infinity without sharing their energy with the stellar-envelope gas (unless their spectrum is strongly modified by coronal processes, see Ramirez-Ruiz & Socrates 2005). Magnetic fields, on the other hand, couple to the gas tightly

<sup>1</sup> Princeton University, Department of Astrophysical Sciences, Peyton Hall, Princeton, NJ 08544 — Center for Magnetic Self-Organization (CMSO); uzdensky@astro.princeton.edu.

<sup>2</sup> Institute for Advanced Study, Princeton, NJ 08540; aim@ias.edu.

and this makes them a very efficient explosion agent. Energetically, magnetic GRB models are usually quite plausible. For example, assuming a typical surface magnetic field  $B_* = 10^{15}$  G, a rotation rate  $\Omega_* = 10^4$  sec $^{-1}$ , and a radius  $R_* = 10$  km, it is easy to see that the resulting basic energetics and timescales fall just in the right ballpark to make the millisecond magnetar a plausible candidate for a GRB central engine (e.g., Thompson 1994). Indeed, the total rotational energy of a millisecond-period neutron star is  $E_{\text{rot}} \simeq 5 \cdot 10^{52}$  erg, which is more than enough to drive a long-duration GRB. The time scale for the energy extraction can be estimated by dividing this available energy by the total magnetic luminosity (the spin-down power),  $L_{\text{magn}}$ . The latter can be roughly estimated by the usual pulsar luminosity formula  $L_{\text{magn}} \sim B_*^2 R_*^6 \Omega_*^4 c^{-3}$ , which for the above parameters yields  $\sim 3 \cdot 10^{50}$  erg sec $^{-1}$ , corresponding to the characteristic timescale of order 100 sec. Thus, from the point of view of the overall energetics and timescales, the millisecond-magnetar central engine is just a scaled-up version of the Ostriker & Gunn (1971) model for regular pulsar-powered supernovae (with the magnetic field scaled up by three orders of magnitude and the time scaled down by six orders of magnitude).

It has to be noted, however, that the plausible overall energetics and timescales are, by themselves, not sufficient for making a good GRB central engine model. This is because there are some extra physical requirements mandated by observations. In particular, to make a successful GRB, the central engine has to be capable of producing an energetic outflow that is (1) ultra-relativistic; (2) highly-collimated; and (3) baryon-free. The pioneering works cited above have focused mostly on the energetics and timescales, but not on the mechanisms for producing an outflow that satisfies these requirements (see, however, Wheeler et al. 2000 and Bucciantini et al. 2006 for a discussion of collimation). Also, most of these previous models, with the notable exceptions of Wheeler et al. (2000) and Arons (2003), see § 2.3, have considered a magnetar in isolation; that is, they have completely ignored the effect of any surrounding stellar gas on shaping the outflow. This may be a good approximation for the accretion-induced collapse of a white dwarf, but it is not appropriate in the collapsing-star scenario.

In contrast, in this paper we stress that the infalling stellar gas is still present during the explosion and needs to be taken into account. Thus, an important new element that distinguishes our model from those previous works is the consideration of the interaction between a newly-born magnetar and the stellar plasma in which it is initially embedded. Specifically, we argue that the pressure and inertia (i.e., the ram pressure) of the surrounding stellar gas acts as a natural collimator forcing the magnetized outflow into two tightly beamed jets. It also plays a crucial role in magnetic extraction of rotational energy from the magnetar.

In order to illustrate these ideas we introduce the “Pulsar-in-a-Cavity” problem as a basic-physics paradigm for this scenario. We describe this problem in detail in § 2. We first give a general description of the problem and its various versions. Then, in § 2.1, we consider the simplest special case of a rotating force-free magnetosphere inside a fixed rigid cavity. In that section, we first demonstrate that differential rotation of the magnetic field lines is inevitably established inside the cavity, even if the pulsar itself is rotating uniformly; as a result, a strong toroidal magnetic field gradually builds up. We then study the long-term evolution of the magnetic

field inside the cavity and show that the magnetic luminosity increases with time. We also show that a massive, non-force-free plasma strip unavoidably arises in the equatorial plane beyond the light cylinder. In § 2.2 we discuss the subtle issue of hoop-stress collimation and argue that external confinement and differential rotation are two important ingredients for collimating relativistic Poynting-flux dominated outflows. We then consider, in § 2.3, the case of a magnetosphere surrounded by a cavity with a fixed external pressure (instead of a fixed radius).

In § 3 we discuss a specific example relevant to the core collapse of a massive star: a cavity formed behind the stalled bounce-shock at the center of the collapsing star. The radius of the shock stays roughly stationary on the timescale for magnetic fields in the cavity to grow. At the same time, both the ram pressure of the gas falling onto the cavity and the neutrino energy deposition inside it decrease with time. We therefore argue that at some point, a fraction of a second after bounce, the magnetic field will inevitably start to dominate the force balance, leading to a magnetically-driven explosion.

In § 4, we further explore some of the astrophysically-interesting aspects of our model. Thus, in § 4.1, for example, we address an important issue of  $^{56}\text{Ni}$  production and argue that the two-phase nature of the explosion in our model is well-suited to explain a large amount of  $^{56}\text{Ni}$  inferred from observations. In § 4.2 we briefly discuss the possibility of restarting the GRB engine by the fall-back of the post-explosion material. In § 4.3 we describe an extension to our model: a “magnetar-in-a-tube”, motivated by the fact that the material along the rotation axis does not experience a centrifugal barrier and hence falls onto the PNS faster. In section § 4.4 we discuss the implications of our model for pulsar kicks. Finally, in § 4.5, we suggest some directions for future numerical simulations of this problem. We draw our conclusions in § 5.

## 2. THE PULSAR-IN-A-CAVITY PROBLEM

In order to understand how a millisecond magnetar central engine operates in the collapsar context, it is first necessary to consider the following basic physics problem: what happens when an axisymmetric pulsar is placed inside a conducting cavity filled with a low-density infinitely-conducting plasma (see Fig. 1)? Specifically, we are interested in a situation where the cavity radius  $R_0$  is much larger than the pulsar light-cylinder radius  $R_{\text{LC}}$ . We call this idealized problem the *Pulsar-in-a-Cavity problem* (Uzdensky & MacFadyen 2006) and we propose it as the first essential step in building up a physical understanding of the problem. It is a modification of the famous problem of an axisymmetric rotating magnetic dipole in free space, considered by Goldreich & Julian (1969) as a model for an isolated pulsar’s magnetosphere. In some aspects, it is also similar to the system considered by Kardashev (1970), Ostriker (1970; unpublished), and by Ostriker & Gunn (1971).

We would like to point out that adding a cavity makes the problem, in a sense, less fundamental since the behavior of the system depends, in general, on the assumed physical properties of the cavity. To make the situation less arbitrary, we shall fix the electromagnetic properties of the cavity by assuming that its walls are perfectly conducting, as is the plasma that fills the cavity. We shall also assume that all the field lines close back to the pulsar inside the cavity, i.e., that there are no field lines connecting the pulsar to the cavity wall. This choice is most natural when the bulk of the magnetic flux has

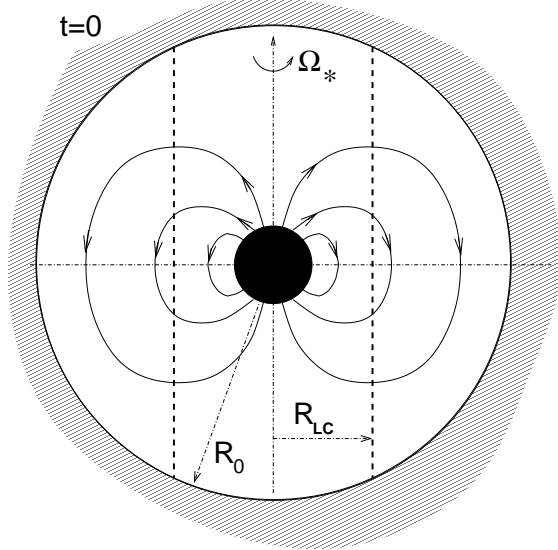


FIG. 1.— An aligned pulsar inside an infinitely-conducting spherical cavity of radius  $R_0$  at  $t = 0$ . The vertical dashed lines represent the pulsar's light cylinder of radius  $R_{LC} < R_0$ .

been produced by a dynamo operating inside the neutron star and then emerged through its surface (as is in the case of magnetars), as opposed to a situation where the pulsar field lines connect directly to the wall (i.e., to the outer stellar envelope, as considered, e.g., by Kardashev 1970 and by Goldreich et al. 1971). At the same time, we are still left with a lot of freedom regarding the mechanical properties of the cavity. Thus, we are dealing not with one unique problem, but instead with a whole class of problems. Correspondingly, we propose that the overall problem be treated as a sequence of test problems with increasingly more sophisticated treatment of the cavity boundary. Depending on the physical situation, this sequence may also represent various stages in the time evolution of the system.

For example, one can first consider the case where the cavity walls are rigid and have a fixed (e.g., spherical) shape (see § 2.1). This may represent the early stages of the system's evolution. Next, one can assume that the shape and the size of the cavity are not fixed but instead are governed by the pressure balance between the electro-magnetic stress inside the cavity and a constant external pressure outside (see § 2.3). This makes the set-up similar to Lynden-Bell's (1996) magnetic tower model. Thirdly, one can consider a pulsar in a fully dynamic environment of a collapsing star. The set-up of the latter problem is essentially similar to that considered by Ostriker & Gunn (1971).

All three versions of our pulsar-in-a-cavity problem are basic physics problems that ought to be solved if we are ever to understand how a millisecond magnetar works inside a collapsing star. Our understanding of these problems will benefit from rigorous mathematical analysis, but ultimately will most likely be achieved with the help of numerical simulations that are now becoming feasible. Whereas the first two problems represent perfect targets for relativistic force-free simulations, the third problem will most likely require a full relativistic MHD simulation.

In order to set the stage for future numerical studies, and to be able to interpret their results, it is useful to get some basic qualitative understanding of the problem. Therefore, in

this section we will sketch what we think is a plausible physical picture of the system's evolution and how it relates to our magnetic tower model for GRBs (Uzdensky & MacFadyen 2006).

In order to gain a more complete understanding of the interaction between the central magnetar and the surrounding stellar material, a full magnetohydrodynamic (MHD) description that includes plasma pressure and inertial effects will eventually be required. Of particular interest would be the confinement of the expanding magnetosphere by the surrounding plasma and the dynamical response of the star to the expanding magnetosphere at its center. The full-MHD approach is especially relevant if there is a strong wind driven off the PNS by neutrinos and/or by the magneto-centrifugal mechanism, as considered by Thompson et al. (2004) and by Bucciantini et al. (2006). A useful simplification may come from noting that the main difference between the dense-plasma case and the relativistic force-free case is just the difference between the Alfvén speed and the speed of light (J. Ostriker, private communication). Then, the MHD case may be treated similarly to the relativistic force-free case, but with the light cylinder replaced by a smaller Alfvén surface.

For simplicity, however, in this paper we shall restrict ourselves to the force-free case. That is, we shall assume that the plasma density inside the cavity is so low that electromagnetic forces dominate the dynamics almost everywhere inside the cavity (but outside the neutron star of course). The only exception is the part of the equatorial plane outside the light cylinder, where plasma inertia needs to be taken into account (see below). While not realistic, given the large plasma densities present in the center of a massive star, the force-free description may nonetheless reflect some essential features of the full solution. It is of relevance especially for late phases of the evolution when the magnetic field outside the neutron star has been amplified to large values.

As we have already mentioned, we shall also assume that the plasma inside the cavity can be accurately represented by an infinitely conducting fluid. We expect this key assumption to be well justified throughout most of the cavity, owing to the very large plasma densities and temperatures. Indeed, the high plasma density ensures that the plasma (including photons) is highly collisional and hence is well described by resistive MHD; this means that the resistivity due to particle-particle or photon-particle collisions dominates over all other non-ideal terms in generalized Ohm's law. On the other hand, because of the very high plasma temperature, the resistivity is actually quite small, i.e., the magnetic Reynolds number is very high. All this makes ideal MHD a good approximation in the environment of a collapsing star (see Uzdensky & MacFadyen 2006 for more discussion). At the same time, we do acknowledge that this assumption may break down in some special regions, in particular, inside the equatorial plasma strip (see below) and at the cavity boundary, where various fluid instabilities may lead to enhanced turbulent energy dissipation. In any case, however, we expect ideal MHD to be much better justified inside a collapsing star than the force-free assumption. For this reason, in this paper we shall ignore any finite-resistivity effects, leaving them for a future study.

Throughout most of this discussion we shall ignore all numerical factors, e.g.,  $4\pi$ , etc. Also, we shall assume that the magnetar rotation rate  $\Omega_*$  stays approximately constant on the timescales under consideration. However, ultimately one will have to consider the effect of decreasing rotation rate as the

pulsar slows down.

Finally, we would like to stress that there are important differences between the problem of an isolated pulsar magnetosphere and our pulsar-in-a-cavity problem. In particular, in the isolated pulsar case one usually seeks a steady state (although perhaps employing time-dependent simulations to achieve it). In the pulsar-in-a-cavity case, on the other hand, we don't expect a stationary solution; the problem is intrinsically time-dependent and it is the time evolution of the system that is of particular interest.

### 2.1. Pulsar in a Fixed Spherical Cavity

We start with our problem I, in which the walls of the cavity are fixed. For definiteness, we take the cavity to be spherical in shape. The main results obtained in this section should also be approximately valid for the case of expanding (or contracting) cavity, as long as the expansion (contraction) speed is slow compared with the speed of light.

Let us try to think physically about how the magnetic field will evolve after the pulsar is spun-up instantaneously at  $t = 0$ . In the isolated pulsar case, the field lines extending beyond the light cylinder bend backwards and become open (Goldreich & Julian 1969). Then, the pulsar continuously spins down, losing its rotational energy and angular momentum to magnetic braking by these open field lines. In our case, on the other hand, such an immediate field-line opening is not possible since the entire magnetosphere is contained inside the cavity.

In the Goldreich–Julian (1969) model for an isolated pulsar, the field lines actually also close, very far away, in the so-called “boundary zone”. But as long as the cavity (the outer edge of the magnetosphere) expands faster than the fast magnetosonic speed, there is no feedback of this boundary on the inner magnetosphere. This is the one critical difference with our case.

#### Development of Differential Rotation

One important point that one needs to take into account is the establishment of *differential rotation* in the magnetosphere. This is nontrivial, since, by assumption, the magnetar rotates uniformly. However, as we will now show, the field lines that extend beyond the pulsar light cylinder nevertheless necessarily undergo differential rotation. As a result, these field lines are continuously twisted and hence toroidal flux is continuously injected into the cavity.

To see how this comes about, let us consider a field line  $\Psi$  (Fig. 2) and compare the angular velocities at two points on this line: point  $A$ , where the field line attaches to the pulsar, and point  $B$ , where it intersects the equator. Since this field line extends beyond the light cylinder, it cannot remain purely poloidal: toroidal field has to develop so that the plasma particles could slide backwards and out along the line, like beads on a wire. This toroidal field leads to a continuous braking of the star so that there is an outward flux of angular momentum and a Poynting flux of energy along the line. However, the toroidal magnetic field at point  $B$  has to be exactly zero because of the assumed reflection symmetry with respect to the midplane. Therefore, the plasma can no longer slide toroidally; this means that the toroidal velocity of the field line is equal to that of the plasma at this point. The angular momentum and rotational energy of the pulsar extracted by the magnetic field are partly accumulated and stored in the magnetic form and partly transferred to the equatorial plasma. Thus, the material at point  $B$  is continuously torqued by the

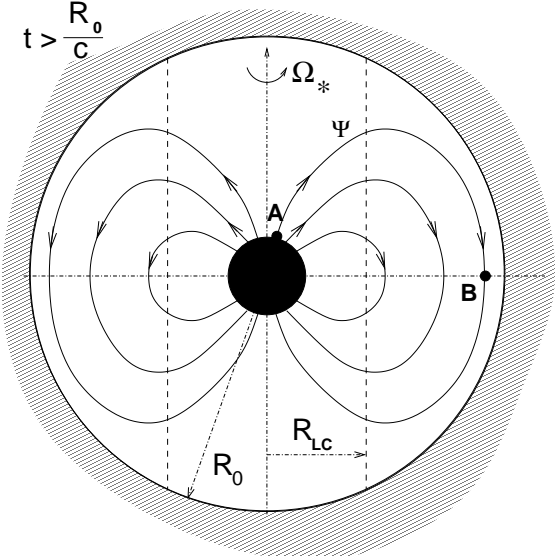


FIG. 2.— An aligned pulsar inside an infinitely-conducting spherical cavity of radius  $R_0$ . After a time of order the light-crossing time  $R_0/c$ , the poloidal field lines outside the light cylinder expand somewhat but still remain confined within the cavity. Because the toroidal magnetic field has to vanish at the equatorial midplane due to reflection symmetry, the field lines there cannot corotate with the star,  $\Omega_B < c/R_B < \Omega_*$ . As a result, differential rotation is established in both hemispheres,  $\Delta\Omega = \Omega_* - \Omega_B \simeq \Omega_*$  (for  $R_B \gg R_{LC}$ ), which leads to continuous generation of toroidal magnetic flux.

magnetic field. Then, since the confining wall prevents the material from moving out freely in the radial direction, the toroidal velocity of the plasma becomes closer and closer to the speed of light. However, it can never exceed the speed of light; therefore, the plasma, and hence field-line, angular velocity at point  $B$  is bounded:  $\Omega_B \simeq c/R_B = \Omega_* R_{LC}/R_B$ . On the other hand, the angular velocity at point  $A$  is of course just the rotation rate of the pulsar:  $\Omega_A = \Omega_*$ . This means that the field line experiences differential rotation at a rate  $\Delta\Omega = \Omega_A - \Omega_B \geq \Omega_*(1 - R_{LC}/R_B)$ . For field lines that cross the equator well outside the light cylinder,  $R_B \gg R_{LC}$ , we then have  $\Delta\Omega \approx \Omega_*$ . Thus, differential rotation is established over a time-scale of order the light-crossing time across the cavity,  $t_0 \equiv R_0/c \gg \Omega_*^{-1}$ .

This differential rotation is important because it leads to a continuous toroidal stretching of the field lines and thus to a continuous injection of toroidal magnetic flux (of opposite signs) into the upper and lower hemispheres. Since all this toroidal flux has to be contained within a cavity of fixed size, the toroidal magnetic field at any given point grows, roughly speaking, linearly in time. This is in contrast with the pulsar in a free space, where, within a sphere of any given radius, a steady state is established on the time scale of order the light travel time across this radius.

The toroidal field reverses sharply across the equator, so there is a non-force-free equatorial current sheet that carries the radial return current back to (or from) the neutron star (see below).

#### Magnetic field structure at late times

Now let us try to estimate the toroidal field evolution and distribution inside the cavity on long time scales ( $t \equiv Nt_0$ , where  $N \gg 1$ , and  $t_0 \equiv R_0/c$  is the light crossing time across the cavity) and at distances much larger than the light cylinder radius.

As we discussed above, because of the differential rotation, the bounded magnetosphere cannot be stationary: toroidal magnetic flux is constantly being injected into a finite volume. Hence, the toroidal field strength continuously increases, whereas the poloidal magnetic field does not. The poloidal electric field,  $E_{\text{pol}}$ , may become much larger than  $B_{\text{pol}}$  but in any case cannot exceed the value  $B_{\text{pol}}\Omega_*R_0/c = B_{\text{pol}}R_0/R_{\text{LC}}$ . Thus, after several light-crossing times the magnetosphere outside the light cylinder becomes toroidal-field dominated:  $B_\phi \gg E_{\text{pol}}, B_{\text{pol}}$ .

Next, even though the configuration is time-dependent, after many light-crossing times the evolution slows down. Indeed, the poloidal field structure readjusts (e.g., in response to a change in the toroidal field strength) on a time scale of order the fast-magnetosonic crossing time across the cavity; for a force-free plasma this coincides with  $t_0 = R_0/c$ . Since the toroidal flux grows linearly in time, the relative change in the toroidal field strength over  $\Delta t \sim t_0$  becomes small (of order  $N^{-1}$ ) at late times,  $t = Nt_0$ ,  $N \gg 1$ . An approximate force-free equilibrium is then established separately in each of the two hemispheres, with poloidal current being approximately constant on poloidal flux surfaces:  $I \simeq I(\Psi)$ . The magnetic field structure in such an equilibrium is governed by the relativistic force-free Grad–Shafranov equation (aka the pulsar equation). In the limit where the toroidal magnetic field totally dominates the dynamics, this equation reduces to  $II'(\Psi) = 0$ , so that the poloidal current function becomes independent of  $\Psi$ :  $I(\Psi) = I_0 = \text{const}$ . This corresponds to the vacuum field produced by a singular line current  $I_0$  (which grows linearly in time) flowing along the rotation axis. The toroidal magnetic field is  $B_\phi(t, R, Z) = I_0(t)/R$ , i.e.,  $B_\phi = \text{constant}$  on cylinders, and the equilibrium can be described as the balance between the toroidal field tension and pressure. In other words, the  $\mathbf{j} \times \mathbf{B}$  force becomes relatively small inside the cavity, because the poloidal current becomes spatially separated from the toroidal magnetic field: it flows out of the pulsar along the axis (in both hemispheres), then as a surface current along the cavity walls, and finally returns to the pulsar along the non-force-free equatorial current sheet. The bulk of the magnetosphere is thus almost current-free. In this regard, the electric-current structure of the cavity is similar to that of the magnetic bubble considered by Lyutikov & Blandford (2002, 2003) in their model for Poynting-flux dominated GRB outflows (although we apply our model deep inside the collapsing star, that is, on different spatial and temporal scales compared with their model).

Let us now estimate the magnitude of the poloidal line current  $I_0(t)$  and hence the characteristic strength of the toroidal field in the cavity. We shall express magnetic quantities characterizing the field in the cavity in terms of the total poloidal magnetic flux that extends beyond the light cylinder, which we shall call  $\Psi_0$ . Up to a factor of order unity, this flux can be estimated from the pure dipole magnetic field, i.e.,

$$\Psi_0 \sim \Psi_{\text{dipole}}(R_{\text{LC}}) = B_* \frac{R_*^3}{R_{\text{LC}}}. \quad (1)$$

This estimate is justified because inside the light cylinder the poloidal field remains close to dipole. Moreover, even in the extreme case of an unbounded, isolated pulsar magnetosphere, in which the field is completely open outside the light cylinder, the poloidal flux crossing the light cylinder differs from the dipole formula only by a small amount (e.g., Contopoulos, Kazanas & Fendt 1999; Komissarov 2006; McKinney 2006b; Spitkovsky 2006). Thus, this estimate should be

quite good in our case as well.

Now, what is the characteristic poloidal magnetic field strength in the cavity at distances  $r \sim R_0$ ? Here the dipole formula ( $B_{\text{pol}} \sim r^{-3}$ ), describing a fully-closed non-rotating field, and the split-monopole formula, describing the fully-open magnetosphere of an isolated pulsar, differ. In our case, all the field lines are closed, i.e., they intersect the equator within  $R_0$ , so one might think that the dipole-field estimate should be more applicable. However, as we show below, almost all of the field lines crossing the light cylinder actually intersect the equator in a narrow strip near the outer wall; therefore, the characteristic poloidal field at distances of order  $R_0$  from the center and off the equatorial plane should be estimated as

$$B_{\text{pol}} \sim B_0 \equiv \frac{\Psi_0}{R_0^2}. \quad (2)$$

For  $\Psi_0$  given by equation (1), this estimate gives a value  $B_{\text{pol}} \sim B_*(R_*^3/R_*^2 R_{\text{LC}})$ , which is by a factor  $R_0/R_{\text{LC}}$  larger than a pure dipole field at these distances.

Now let us estimate the poloidal current and the toroidal magnetic field. In general, the poloidal current flowing through a region enclosed by an axisymmetric flux surface  $\Psi$  can be calculated by following the shape of a field line corresponding to  $\Psi$ :

$$I(\Psi, t) = \Delta\Omega t \left[ \int_{\Psi} \frac{dl_{\text{pol}}}{B_{\text{pol}} R^2(l_{\text{pol}})} \right]^{-1}, \quad (3)$$

where  $l_{\text{pol}}$  is the path-length along the poloidal field. The main contribution to the integral comes from large distances,  $R \sim R_0$  and thus the integral can be estimated as being of order  $R_0/\Psi_0$ . Then, since  $\Delta\Omega \simeq \Omega_* = c/R_{\text{LC}}$ , the axial poloidal current can be estimated as

$$I_0(t) \sim \Omega_* t \frac{\Psi_0}{R_0} \simeq \frac{\Psi_0}{R_{\text{LC}}} \frac{t}{t_0}. \quad (4)$$

Thus we see that for  $t \gg t_0$  the poloidal current becomes much stronger than the typical poloidal current in the unbounded pulsar magnetosphere ( $I \sim \Psi_0/R_{\text{LC}}$ ). Using the estimate (1) for  $\Psi_0$ , we can express  $I_0$  as

$$I_0(t) \sim B_* \frac{R_*^3}{R_{\text{LC}}^2} \frac{t}{t_0}. \quad (5)$$

Correspondingly, the characteristic toroidal magnetic field at distances of order  $R_0$  is

$$B_\phi(R_0) = \frac{I_0}{R_0} \simeq B_0 \Omega_* t, \quad (6)$$

which is similar to the estimate presented by Kardashev (1970) for the toroidal field of a pulsar inside an expanding supernova cavity. We see that, after many light-crossing times across the cavity,  $B_\phi(R_0)$  becomes much larger than the toroidal field of an isolated pulsar at these distances [ $B_\phi^{\text{isolated}} \sim \Psi_0/(R_0 R_{\text{LC}}) = B_0(R_0/R_{\text{LC}}) = B_0(R_0/R_{\text{LC}}) \ll B_0 \Omega_* t$ ].

Finally, we would like to remark on how to determine the structure of the poloidal field,  $\Psi(r, \theta)$ . Usually, when studying steady-state axisymmetric magnetospheres, one uses an iterative procedure (e.g., Contopoulos et al. 1999). First, one makes a guess for the poloidal current  $I(\Psi)$ , plugs it into the Grad–Shafranov equation, and solves this equation for  $\Psi(r, \theta)$ . Then one uses equation (3) to determine the new function  $I(\Psi)$  and repeats the steps until the procedure converges. In our case, however, this approach does not appear to

be feasible, since to lowest order the Grad–Shafranov equation simply gives  $I(\Psi) = I_0 = \text{const}$ . We therefore advocate for an inverted approach where the poloidal flux function is determined from equation (3). How to realize such an approach in practice is not clear. One thing to note though is that this calculation should depend on  $\Psi(R, Z=0)$  as a boundary condition, and this has to be determined from considering the redistribution of the poloidal flux across the equatorial midplane. This issue is discussed in the next subsection.

### Centrifugal Force in the Equatorial Plane

As we noted above, the magnetosphere outside the pulsar light cylinder cannot be entirely force-free. Because the toroidal magnetic field reverses across the equator (due to the assumed reflection symmetry), the magnetic field tension continuously accelerates the equatorial plasma in the toroidal direction. Correspondingly, this tension force performs mechanical work on the equatorial plasma and so a certain part of the rotational energy extracted from the pulsar by the magnetic field is deposited in the equatorial plane (the rest is stored in the bulk of the cavity as the toroidal magnetic field energy). Since the plasma in the equatorial plane rotates ultra-relativistically, the added energy leads to an increase in the relativistic “mass” of the plasma,  $\Delta m \sim t^2$ . An important consequence is that this relativistically-rotating massive equatorial sheet experiences an outward radial centrifugal force,  $F_{\text{cent}}$ . This force cannot be balanced by the toroidal magnetic field because the latter is zero at the equator. Consequently, the equatorial plasma moves towards the wall and compresses poloidal magnetic field, until finally the centrifugal force is balanced by the  $\mathbf{j} \times \mathbf{B}$  force due to the non-force-free part of the toroidal current  $j_\phi$ .<sup>3</sup> Thus, the poloidal magnetic flux in the equatorial plane outside the light cylinder is pushed against the wall and is strongly concentrated in a narrow band of ever-decreasing width  $d(t) \ll R_0$  near the wall (see Fig. 3). Because of this effect, we can expect nearly all the poloidal flux  $\Psi_0$  that extends beyond the light cylinder to cross the equator inside this strip, i.e., at cylindrical radii  $R \simeq R_0$ . At the same time, in the magnetosphere above and below the equatorial plane, the poloidal field lines that emanate from this band have to fan out because they have to fill the cavity volume. Thus, the characteristic poloidal magnetic field in the cavity is of the order  $B_0 = \Psi_0/R_0^2$  (see eqn. 2) and is much weaker (by a factor of  $d/R_0$ ) than in the equatorial strip.

Let us assess the centrifugal force quantitatively. The total torque exerted on the massive equatorial strip by the magnetic field is given by  $\tau(t) = \int I(\Psi, t) d\Psi \simeq I_0(t) \Psi_0$ . Since the toroidal velocity of this strip is close to the speed of light, the total work per unit time due to this torque (i.e., the total Poynting flux that arrives at the strip) is  $P_{\text{strip}} \simeq \tau c/R_0 = B_\phi c \Psi_0$ . This power goes into accelerating the rotation of plasma in the strip, and some part of it may in principle be dissipated into heat. Since the rotation here is already ultra-relativistic, the result of this acceleration is an increase in the rotation and/or thermal  $\gamma$ -factors, i.e., of the relativistic mass  $m$  of the plasma in the strip:  $d/dt(mc^2) = P_{\text{strip}}$ . As a result, the relativistic mass grows with time as

$$m(t)c^2 \sim \Omega_*^2 t^2 \frac{R_{\text{LC}}}{R_0} \frac{\Psi_0^2}{R_0} \sim \left(\frac{t}{t_0}\right)^2 \frac{R_0}{R_{\text{LC}}} \frac{\Psi_0^2}{R_0} \sim \frac{R_{\text{LC}}}{R_0} B_\phi^2(t) R_0^3, \quad (7)$$

<sup>3</sup> The contribution from the force-free part,  $j_\phi^{\text{ff}}(z=0) = \rho_e v_\phi(z=0)$  is exactly canceled by the radial electric force,  $\rho_e E_r$ , provided that the ideal-MHD condition  $c\mathbf{E} = \mathbf{v} \times \mathbf{B}$  holds in the equatorial strip.

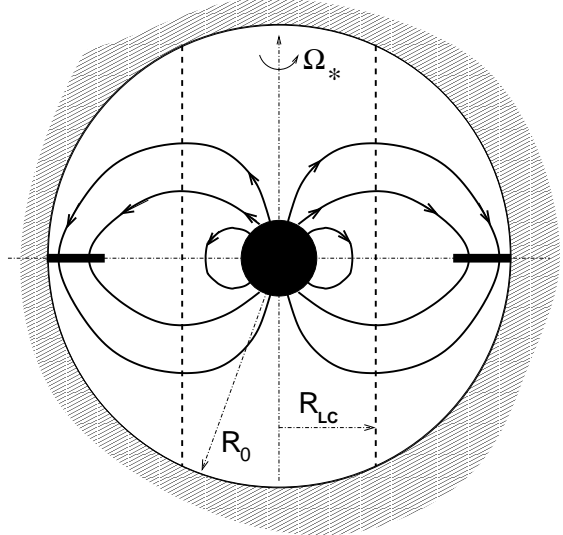


FIG. 3.— At late times, the poloidal magnetic field is pressed against the wall by the centrifugal force of the rotating massive equatorial sheet.

that is, the plasma energy in the equatorial strip always remains small compared with the energy  $B_\phi^2(t)R_0^3$  stored in the toroidal magnetic field at these distances. The centrifugal force acting on the equatorial strip can be estimated as

$$F_{\text{cent}}(t) = \frac{m(t)c^2}{R_0} \sim B_0^2 R_0^2 \Omega_*^2 t^2 \frac{R_{\text{LC}}}{R_0} \sim B_\phi^2(t) R_0^2 \left(\frac{R_{\text{LC}}}{R_0}\right). \quad (8)$$

We see that this force grows quadratically with time, just as the toroidal field pressure, but always remains small (by a factor of  $R_{\text{LC}}/R_0 \ll 1$ ) compared with the overall horizontal force exerted on the side wall by the toroidal field.

A detailed analysis of the internal structure of the massive equatorial plasma strip, including its vertical structure, lies beyond the scope of this paper. However, we present here a simple estimate for the Lorentz factor due to rotation,  $\gamma_{\text{rot}}$ , in terms of the strip width  $d$  and half-thickness  $h$ . This estimate is derived under a certain very restrictive set of assumptions and serves for illustration only.

Let us consider the vertical force balance inside the strip in the co-rotating frame, and let us neglect the contribution from electric force for simplicity. Then the toroidal magnetic field pressure outside the strip has to be balanced by the plasma pressure inside:  $p_{\text{co}} = B_\phi^2/8\pi$ . Next, let us make the assumption that the plasma in the strip is a light relativistic fluid with the adiabatic index 4/3. Then, the co-moving energy density is  $\rho_{\text{co}} c^2 = 3p_{\text{co}}$ . On the other hand, the total plasma energy  $mc^2$  inside an annular strip of radius  $R_0$ , width  $d$ , and thickness  $2h$  can be written in the lab frame as  $mc^2 = 4\pi R_0 dh \rho_{\text{co}} c^2 \gamma_{\text{rot}}^2$ . By combining all these expressions with the equation (7) for  $mc^2$ , we find

$$\gamma_{\text{rot}}^2 \sim \frac{2}{3} \frac{R_0 R_{\text{LC}}}{dh}. \quad (9)$$

On the other hand, it may be possible that a significant amount of plasma accumulates in the equatorial strip or that the plasma there is strongly compressed by the toroidal field pressure. Then, the baryon number density  $n_b$  may become so large that the co-moving energy density is dominated by the non-relativistic component, i.e., by the baryon rest-mass,  $\rho_{\text{co}} c^2 \simeq n_b c m_p c^2 \gg p_{\text{co}} = B_\phi^2/8\pi$ . Since  $n_{b,\text{co}} = \gamma_{\text{rot}}^{-1} n_b$ , the

condition that this is true can be written as

$$\gamma_{\text{rot}}^{-1} \gg \sigma \equiv \frac{B_\phi^2}{4\pi n_b m_p c^2}. \quad (10)$$

Provided that we are in this regime, the total plasma energy in the strip is dominated by the kinetic energy of the baryons:  $mc^2 = 4\pi R_0 dh \gamma_{\text{rot}} n_b m_p c^2$ . Then, using equation (7), we get

$$\gamma_{\text{rot}} \sim \frac{R_0 R_{\text{LC}}}{dh} \sigma_{\text{strip}}, \quad (11)$$

By substituting this expression into the condition (10), we see that the co-moving energy density is dominated by the rest-mass of the baryons only when

$$\sigma \ll \sqrt{\frac{dh}{R_{\text{LC}} R_0}} \ll 1. \quad (12)$$

Correspondingly, we have

$$\gamma_{\text{rot}} \ll \sqrt{\frac{R_0 R_{\text{LC}}}{dh}}. \quad (13)$$

### Magnetic Spin-down Power of a Pulsar in a Fixed Cavity

Another extremely important point is that the rate at which the magnetic field in a bounded magnetosphere extracts rotational energy from the central rotating conductor actually grows with time. This is because the magnetic torque per unit area is proportional to the toroidal field at the conductor's surface and the latter grows linearly with time. Thus, the magnetic power generated by a spinning pulsar inside a cavity increases linearly with time as long as the cavity does not expand (or expands slowly) and the spin rate of the pulsar stays constant. We can estimate the spin-down power as

$$P(t) = I(t) \Psi_0 \Omega_* = \Omega_*^2 t \frac{\Psi_0^2}{R_0} \sim P_{\text{isolated}} \frac{ct}{R_0}, \quad (14)$$

where  $P_{\text{isolated}} \sim B_*^2 R_*^6 \Omega_*^4 / c^3$  is the spin-down power of an isolated, unbounded pulsar. As we see, after many light-crossing times, the power of a pulsar-in-a-cavity greatly exceeds that of a classical isolated pulsar. This is our answer to the apparent paradox raised by Lyutikov (2006).

We thus emphasize that the energy extraction from a magnetar-in-a-cavity can be a run-away process. This is because the twisting of a magnetic field confined by an external boundary results in an increase in the field's strength at the light cylinder and hence in a growing rate of energy extraction from the magnetar.

This effect can be attributed to a positive feedback that exists between the energy that has been already extracted from the pulsar, and the strength of the agent that extracts the energy (the toroidal magnetic field). Namely, most of the extracted energy is stored in the toroidal magnetic field, and since the volume occupied by this field is kept finite, the toroidal field strength increases with time. Because the magnetosphere remains in a quasi-equilibrium, the toroidal field constantly readjusts everywhere, including within the light cylinder. In other words, because the system is not hyperbolic but elliptic, the inner magnetosphere feels the presence of the outer confining wall. In particular, the toroidal field at the very surface of the pulsar increases linearly with time, and hence so does the spin-down torque exerted by the magnetic field on the pulsar. This picture is similar to what is happening in the combustion chamber of a rocket, for example. In that case, the gas temperature and pressure increase

as the chemical energy of the fuel is released in the combustion process. At the same time, the rate at which fuel burning occurs increases with an increase in the ambient temperature. As a result, rapid and efficient burning demands high pressure and hence a strong confining chamber capable of withstanding this pressure. Similarly, in our case of a pulsar placed inside a cavity, the presence of strong cavity walls leads to an increased energy extraction rate from the pulsar.

### 2.2. Hoop-stress collimation: contrast with the isolated pulsar

The toroidal field generated by the differential rotation exerts a constantly-growing pressure on the cavity walls. If we now relax the assumption that the walls are fixed and allow them to move, this pressure will make the cavity inflate. We then want to understand how rapidly such inflation will proceed and whether it will be isotropic or, say, collimated along the axis. We discuss the collimation issue in this subsection.

Generally speaking, since the toroidal field pressure in the lateral direction is partly negated by the field's tension (the hoop stress), which has no vertical component, one may expect the resulting expansion to be predominantly vertical. However, notice that here we are interested in a situation where the (differential) rotation is relativistic:  $\Delta\Omega R_0 \sim \Omega_* R_0 \gg c$ . On the other hand, Lynden-Bell's (1996) magnetic tower model, for example, was developed for the non-relativistic regime. It is well-known that hoop-stress collimation is not a trivial issue in the relativistic case. Thus, it is not immediately obvious that the hoop-stress collimation mechanism can be applied to the pulsar-in-a-cavity scenario considered in this paper. We therefore would like to discuss this issue in some detail here.

At first, one might think that there should be no problem collimating the outflow: the magnetic field is predominantly toroidal even without differential rotation. And it is the toroidal field's hoop stress that is usually credited for collimating astrophysical jets. However, as is well known, hoop-stress collimation does not work as well when applied to ultra-relativistic magnetically-dominated outflows, as it does in the non-relativistic case. The quintessential example of this lack of collimation is the isolated-pulsar wind inside the termination shock. The basic reason for this difficulty is the decollimating force due to the poloidal electric field,  $E_{\text{pol}}$ . Indeed, in the case of an *unbounded* relativistic uniformly-rotating force-free magnetosphere (e.g., an isolated aligned pulsar magnetosphere) in a steady state, the poloidal electric and toroidal magnetic fields have to be nearly equal in strength at large distances from the central axis (Goldreich & Julian 1969). Importantly, it turns out that this balance can be realized in an uncollimated, quasi-spherical poloidal magnetic field configuration; an excellent example of this is Michel's (1973) split-monopole solution. A rough argument explaining this lack of hoop-stress collimation in the relativistic-rotation case goes as follows. Let us consider an uncollimated field configuration; the poloidal magnetic field is open outside the light cylinder and has a split-monopole geometry, i.e., drops off with distance as  $r^{-2}$ . In a steady state, the poloidal electric field is  $E_{\text{pol}} = B_{\text{pol}} R / R_{\text{LC}}$  where  $R$  is the cylindrical radius. It therefore drops off along radial rays as  $r^{-1}$ . But the toroidal magnetic field also drops off as  $r^{-1}$ . Moreover, at the light cylinder  $E_{\text{pol}}$  and  $B_\phi$  are comparable:  $E_{\text{pol}} = B_{\text{pol}} \sim B_\phi$ . Since outside the light cylinder they both decrease as the same power of  $r$ , they remain comparable to each other (both being much larger than  $B_{\text{pol}}$ ) at large distances. Moreover, as Goldreich & Julian

(1969) showed,  $E_{\text{pol}}$  and  $B_{\phi}$  even become equal asymptotically as  $r \rightarrow \infty$ . The bottom line is that a quasi-spherical relativistic force-free equilibrium can be established as a balance between the collimating pinch force (the sum of the toroidal magnetic field pressure and its tension) and the opposing electric force. Hoop-stress collimation is suppressed as a result of this balance.

Now, in the case of a rotating magnetosphere enclosed inside a rigid cavity of a fixed radius  $R_0 > R_{\text{LC}}$ , the situation is different and hoop-stress collimation can in fact work. Indeed, as we showed above, after many light-crossing times ( $t \gg R_0/c$ ), the toroidal magnetic field filling the cavity becomes stronger than both  $B_{\text{pol}}$  and  $E_{\text{pol}}$ , in contrast to the isolated pulsar case. Moreover, this toroidal field is distributed nonuniformly; it is basically inversely proportional to the cylindrical radius. Correspondingly, the stress exerted by the toroidal magnetic field on the cavity walls is also nonuniform: the magnetic pressure pushing vertically against the top and bottom walls is much higher than the lateral magnetic pressure acting on the side walls. Therefore, if we now allow the cavity to expand under this pressure, we expect any subsequent expansion to be mostly vertical (see Fig. 4), at least as long as the expansion velocity is slow compared with the speed of light. Then we effectively find ourselves in a situation similar to the non-relativistic magnetic tower proposed by Lynden-Bell (1996). We therefore envision that the eventual, long-term result of this process will be the creation of a pair of oppositely-directed magnetic towers (Uzdensky & MacFadyen 2006). The interaction of the expanding towers with the surrounding stellar envelope aids in their confinement, similarly to jet collimation seen in hydrodynamical simulations of the collapsar model (MacFadyen & Woosley 1999; Aloy et al. 2001; MacFadyen, Woosley & Heger 2001; Zhang, Woosley & MacFadyen 2003). In the scenario considered in the present paper, these towers are driven not by a differentially-rotating disk, but by a rapidly-rotating magnetar. This suggests that considering the magnetosphere of a pulsar inside a cylindrical, as opposed to spherical, cavity may represent yet another interesting and important problem for future study (see § 4.3).

An important element in the above discussion is the fact that the electric field is small compared with the toroidal magnetic field. This is directly related to the fact that the toroidal field is generated not as a part of an outgoing large-scale electromagnetic wave driven by the pulsar rotation, but as a result of differential rotation. This observation points to the important role played by *differential* rotation (as opposed to uniform relativistic rotation) in collimating relativistic force-free outflows.

### 2.3. Pulsar magnetosphere confined by a constant external pressure

Let us now consider the case when the pulsar magnetosphere is confined by some fixed and uniform external gas pressure,  $P_{\text{ext}}$ , instead of a cavity of fixed radius  $R_0$ . We are interested in this particular set-up because it is closest to that considered by Lynden-Bell in his original magnetic tower paper (Lynden-Bell 1996), and we here want to compare his non-relativistic disk model with a pulsar in a similar setting.

Like Lynden-Bell, let us assume that the external pressure is weak compared with the magnetic field pressure  $B_*^2/8\pi$  in the immediate vicinity of the rotating conductor. Moreover, because we are interested in exploring relativistic effects, we want our pulsar magnetosphere to be able to expand

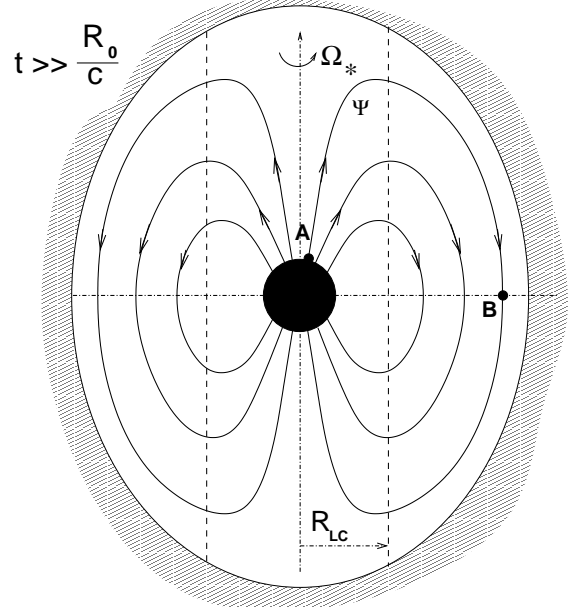


FIG. 4.— Axisymmetric pulsar inside a cavity. After many light-crossing times, the magnetosphere becomes toroidal-field dominated. Because of hoop-stress, the magnetic stress on the cavity becomes strongly concentrated near the axis. This leads to a predominantly vertical, collimated expansion; a magnetic tower forms.

well beyond the light cylinder. Therefore, we shall also assume that the external pressure is small compared with the magnetic pressure of a pure dipole field at the light cylinder:  $8\pi P_{\text{ext}} \ll B_{\text{dipole}}^2(R_{\text{LC}}) \sim B_*^2(R_*/R_{\text{LC}})^6 \ll B_*^2$ .

Let us imagine, as is frequently done in time-dependent pulsar magnetosphere studies (e.g., Komissarov 2006; McKinney 2006b; Spitkovsky 2006), that we start with a non-rotating star with a dipole field and then spin it up suddenly at  $t = 0$ . The initial evolution of the magnetic field is then similar to that of an isolated pulsar: the field lines that extend beyond the light cylinder start to wind up and expand radially at the speed of light, i.e.,  $R_0 \simeq ct$ . This stage of uninhibited quasi-spherical expansion proceeds until the magnetic field pressure at the outer edge of the expanding magnetosphere becomes as small as the external gas pressure. In order to estimate when this happens, we need to evaluate the toroidal magnetic field pressure at  $R = R_0(t)$ . The toroidal field changes with time because of two opposing factors: continuing injection of the toroidal magnetic flux,  $\chi(t) \sim \Psi_0 \Omega_* t = \Psi_0 R_0(t)/R_{\text{LC}}$ , and the increasing volume of the cavity. The net result is that the toroidal field drops off according to

$$B_{\phi}[R_0(t), t] \sim \frac{\chi(t)}{R_0^2(t)} \sim \frac{\Psi_0}{R_{\text{LC}} R_0(t)} \simeq \frac{\Psi_0}{R_{\text{LC}} ct}. \quad (15)$$

Another way to obtain this estimate is to note that the main result of this free expansion is the establishment of the stationary isolated-pulsar magnetosphere inside the radius  $R_0(t)$ . The toroidal magnetic field in an isolated pulsar magnetosphere scales as  $B_{\phi}(r) \sim \Psi_0/R_{\text{LC}} r$  (Goldreich & Julian 1969), which is equivalent to the above estimate.

Eventually, the pressure of the toroidal magnetic field drops to a level where it becomes equal to the external gas pressure (there is also a comparable contribution from the electric field). This happens at time  $t = t_{\text{eq}}$ , corresponding to the cavity

radius reaching an equilibrium value

$$R_{\text{eq}} = ct_{\text{eq}} \equiv \frac{\Psi_0}{\sqrt{8\pi P_{\text{ext}} R_{\text{LC}}}}. \quad (16)$$

After this, the expansion continues, but changes its character: the lateral expansion slows down, and the expansion becomes mostly vertical. Eventually, at  $t \gg t_{\text{eq}}$ , a magnetic tower forms, similar to a linden belltower. One important difference is that since the radius of the tower is much larger than  $R_{\text{LC}}$ , a proper analysis requires relativistic treatment, so Lynden-Bell's non-relativistic theory is not directly applicable. In particular, we expect the vertical expansion of the tower to be relativistic. This can be seen from the following argument. As the tower grows, its radius stays roughly constant, of order  $R_{\text{eq}}$ , whereas its height increases linearly with time, with the velocity  $V_{\text{top}}$ . The continuously injected toroidal flux goes into filling the expanding volume of the tower with toroidal magnetic field, so that, roughly speaking,

$$\chi = \Psi_0 \Omega_* t \sim B_\phi V_{\text{top}} t R_{\text{eq}}. \quad (17)$$

Assuming  $B_\phi \sim \sqrt{8\pi P_{\text{ext}}}$ , we therefore arrive at the estimate

$$V_{\text{top}} \sim c. \quad (18)$$

This result can be understood naturally by noting that the problem has no mass or density parameter and so there is no characteristic velocity scale other than the speed of light  $c$  (scales like  $\Omega_* R_{\text{eq}}$  are even larger than  $c$ ).

The toroidal magnetic field stays roughly constant during this stage, and so the poloidal current flowing through the tower is also constant and is of order

$$I_{0,\text{eq}} \sim B_{\phi,\text{eq}} R_{\text{eq}} \sim \frac{\Psi_0}{R_{\text{LC}}}, \quad (19)$$

the same as the poloidal current in the isolated pulsar case. Correspondingly, the magnetic luminosity (i.e., the spin-down power of the pulsar) stays at a constant level of order  $P_{\text{isolated}}$ . However, unlike the isolated pulsar case, this luminosity is not quasi-spherical, but is channeled predominantly in the vertical direction.

Provided that the expansion of the tower is sub-magnetosonic, an approximate relativistic force-free equilibrium is established inside the tower (at least away from the top lid of the tower). As in the fixed-cavity case, the work done by the toroidal field's magnetic tension on the equatorial current sheet goes into accelerating the equatorial plasma to ultra-relativistic velocities. The relativistic mass of this plasma, and hence also the radial centrifugal force grow linearly with time, as does the overall magnetic pressure force on the outer wall (because of the steadily increasing height of the tower).

As a word of caution, after the toroidal magnetic field becomes dynamically dominant, the resulting equilibrium may become unstable to the sausage and/or kink instabilities. The long-term effect of the nonlinear development of the instabilities is not known at the present and is an important subject for future research.

Another important issue that may potentially plague the development of coherent magnetic structures inside collapsing stars is the development of the Rayleigh-Taylor instability (or its magnetic counter-part, the Kruskal-Schwarzschild instability). In particular, Wheeler et al. (2000) and Arons (2003) pointed out that the interface between the lightweight relativistic fluid (electro-magnetic field and hot relativistic plasma) and the overlying colder, denser stellar material will

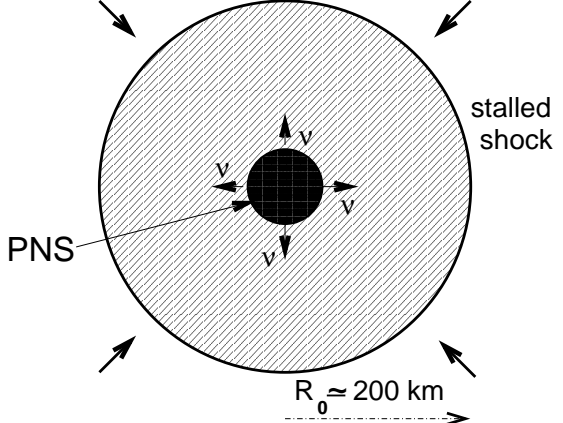


FIG. 5.— The stalled shock phase of core-collapse explosion.

be subject to this instability. In the Arons (2003) model, the stellar envelope is quickly “shredded” by the Rayleigh-Taylor “fingers” that form as a result of the nonlinear development of the instability. This leads to the creation of several evacuated channels that allow the electro-magnetic energy and relativistic particles produced near the central engine to escape through the star. He further argued that these channels suffer only a fairly small amount of mixing with the non-relativistic stellar material due to the Kelvin-Helmholtz instability. In light of this model, we cannot rule out the possibility that our magnetic cavity and/or the subsequently-formed magnetic towers will also fragment into several Rayleigh-Taylor “fingers”. More research is needed in order to asses the implications of this instability for our scenario.

Finally, we would like to reiterate that a proper treatment of these problems requires a time-dependent relativistic force-free or full (preferably relativistic) MHD analysis and simulations (see § 4.5).

### 3. MAGNETAR INSIDE A COLLAPSING STAR: AN OUTLINE OF THE GENERAL SCENARIO

Previous studies of core-collapse supernovae (SNe) have shown that, when the core of a massive star collapses into a proto-neutron star, a bounce shock is launched back into the star (see the reviews by, e.g., Bethe & Wilson 1985; Woosley & Weaver 1986; Bethe 1990). However, as was also shown in these studies, the shock quickly stalls at a radius of about 200 km. The explosion then enters a relatively long ( $\sim 1$  sec) quasi-stationary phase (see Fig. 5). During this phase accreting material constantly moves through the shock and gets heated to very high temperatures. The shock looks stationary in the Eulerian frame and the shock jump condition can be viewed as a balance between the ram pressure of the infalling material, that tends to quench the shock, and the thermal pressure of the post-shocked gas, that is supported mostly by the continuous heating due to neutrino deposition in the dense plasma behind the shock. Gradually, both the neutrino luminosity and accretion rate decline with time. Eventually, one of two things has to happen as an outcome of the competition between neutrinos and accretion. If neutrinos win, the shock engulfs the entire star and one gets a successful SN explosion. If they lose, the shock dies and the PNS gains mass beyond the critical mass and collapses into a black hole, which then subsequently swallows the rest of the star, without a SN.

In our model, we add a third dynamical component — the

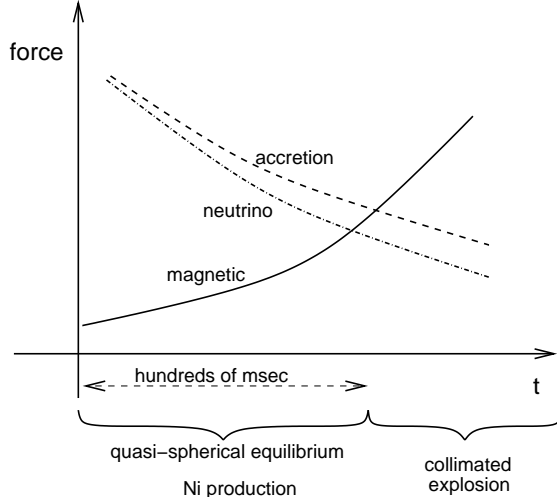


FIG. 6.— Schematic time evolution of the main three forces responsible for the stalled-shock force balance.

magnetic field. The magnetic force is pushing out, helping the explosion, as is the thermal pressure of the neutrino-heated gas. These two outward forces are opposed by the accretion ram pressure. Our main idea is that, generally speaking, the two outward forces evolve differently with time, and thus the explosion may be a two-stage process. In particular, we suggest that the magnetic pressure force is unimportant during the stalled-shock phase that lasts a few hundreds of msec. However, we note that during this time the magnetar makes several hundred revolutions, resulting in a great amplification of the toroidal magnetic flux by the differential rotation. [Of course, during this stage the field is not force-free, and the gas pressure and inertia are important.] Over time, however, both the neutrino energy deposition and the accretion rate decline, whereas the toroidal magnetic field grows (see Fig. 6). For example, assuming  $R_0 = 3R_{LC} = 10R_* = 100$  km, and  $B_* = 10^{15}$  G, we see that the entire cavity is filled with  $3 \cdot 10^{14}$  G fields after about 100 turns (0.1 sec), corresponding to the magnetic pressure of about  $4 \cdot 10^{27}$  erg/cm<sup>3</sup>. This is to be compared with the ram pressure of the infalling stellar material that tries to compress the magnetosphere. The simplest estimate of the ram pressure at  $r = R_0$  is given by

$$P_{\text{ram}} \sim \frac{\dot{M} v_{\text{ff}}}{4\pi R_0^2} \simeq 8 \cdot 10^{27} \dot{M}_0 M_0^{1/2} R_{0,7}^{-5/2} \text{ erg cm}^{-3}, \quad (20)$$

where  $v_{\text{ff}} = (2GM/R_0)^{1/2} \simeq 5 \cdot 10^9 M_0^{1/2} R_{0,7}^{-1/2}$  cm/sec is the free-fall velocity at radius  $R_0$ , and  $M_0$  and  $\dot{M}_0$  are the mass enclosed within radius  $R_0$  and the accretion rate at this radius, expressed in units of  $M_\odot$  and  $M_\odot/\text{sec}$ , respectively. Thus, after a few hundreds of milliseconds, the magnetic pressure overtakes the rapidly decreasing neutrino heating as the main driving force and re-energizes the stalled shock, leading to a successful explosion. This scenario is consistent with the picture presented by Akiyama et al. (2003) who demonstrate numerically the growth of the magnetic field on the 200 msec timescale up to about  $10^{15}$  G in the range of radii up to 100 km. The overall outcome of scenario is also similar to that suggested by Bucciantini et al. (2006), although, because of the winding-up amplification, the magnetic field becomes dynamically important much sooner in our model.

To summarize our picture, the ram pressure of the accreting

material provides a nurturing womb in which the baby magnetic field grows, until it is finally strong enough to break out. Neutrino energy deposition plays an important role during this gestation period, as it provides the support that prevents the magnetosphere from being completely squashed and buried by the accreting gas. Finally, if the above picture is correct and the explosion does become magnetically-driven, then the hoop-stress mechanism makes it highly collimated, thus satisfying one of the key necessary conditions for GRB. Note that this jet is driven by the magnetar-level (i.e.,  $\sim 10^{15}$  G) field and is therefore stronger and faster than the LeBlanc-Wilson (1970) jet that may have been launched a few seconds earlier, during the core-collapse process (Wheeler et al. 2000).

#### 4. DISCUSSION

##### 4.1. Nickel Production

A central issue for the central engine of long-duration GRBs is the required production of  $^{56}\text{Ni}$ . The supernovae that have been observed to accompany long duration GRBs (SN-GRBs) are classified as Type Ibc (SNe Ibc; see, e.g., Soderberg 2006; Kaneko et al. 2006). Modeling of the optical light curves of SNe Ibc requires the presence of radioactive  $^{56}\text{Ni}$  to heat the ejecta after initial post-explosion expansion of the star. The  $^{56}\text{Ni}$  masses inferred from the peak optical brightness of SN-GRBs have a broad range, with the brightest, e.g., SN1998bw and SN2003dh, requiring several  $0.1 M_\odot$ . On average, however, SN-GRBs are not required to produce more  $^{56}\text{Ni}$  than the local population of SNe Ic (Soderberg 2006). In fact, as with low luminosity SNe, e.g., the “tailless” SnII, some GRB-SNe may produce little or no  $^{56}\text{Ni}$  (MacFadyen 2003), as recent observations indicate for GRB060505 and GRB060614, two relatively nearby ( $z \sim 0.1$ ) long GRBs with no detected supernova component (Fynbo et al. 2006; Della Valle et al. 2006; Gal-Yam et al. 2006).

In models of (non-GRB producing) core collapse supernovae,  $^{56}\text{Ni}$  is produced hydrodynamically in material heated to  $T \gtrsim T_{\text{Ni}} \sim 5 \times 10^9$  K by the explosion shock launched in the core of the star. The amount of  $^{56}\text{Ni}$  produced depends on the mass inside of the expanding shock when its temperature declines below  $T_{\text{Ni}}$ . This occurs when its radius has expanded to

$$R_{\text{Ni}} \sim \left( \frac{3E}{4\pi a T_{\text{Ni}}^4} \right)^{1/3} \sim 3.7 \times 10^8 E_{51} \text{ cm}, \quad (21)$$

where  $E = E_{51} \times 10^{51}$  erg is the explosion energy and  $a$  is the radiation constant. The mass inside this radius depends on the density structure of the progenitor star and on how much expansion or contraction occurs before the shock reaches a given mass element. In particular, little or no  $^{56}\text{Ni}$  is produced by a shock, even if extremely powerful, if it is launched into a low density environment. This may occur if a weak initial explosion expands the stellar core so that little mass remains within a few  $10^8$  cm when the strong shock arrives. Production of  $\sim 0.1 M_\odot$  of  $^{56}\text{Ni}$  occurs for many pre-supernova stars if  $\sim 10^{51}$  ergs is deposited isotropically by a (quasi-)spherical shock on a timescale of  $\sim 1$  s so that little pre-expansion of the star occurs before the shock arrives. Some of the brightest supernovae, e.g., SN1998bw, require energies of up to  $\sim 10^{52}$  ergs to make the  $\sim 0.5 M_\odot$  inferred from lightcurve modeling.

The requirement of fast ( $\lesssim 1$  s), isotropic deposition of energy for hydrodynamical production of  $^{56}\text{Ni}$  presents a serious

challenge for models of the SN-GRB central engine. First, because the GRB engine must typically last 10 s or more for relativistic ejecta to escape the star and, second, because GRBs are believed to be highly asymmetric explosions. The high degree of beaming and long timescale for energy deposition renders collapsar jets themselves incapable of producing anywhere near the required  $^{56}\text{Ni}$  masses (MacFadyen & Woosley 1999), since little mass ( $< 0.001 M_{\odot}$ ) can be heated to sufficiently high temperatures. Therefore, in the original collapsar model, with a black hole accretion disk as the central engine, the  $^{56}\text{Ni}$  is produced in a non-relativistic bi-conical wind blown from the disk and constituting a distinct explosion component (MacFadyen & Woosley 1999; MacFadyen 2003).

A fundamental problem for the magnetar model, if it is to produce a GRB and a supernovae, is the requirement that it produce both an isotropic explosion for the  $^{56}\text{Ni}$  production and beamed relativistic ejecta. In our model,  $^{56}\text{Ni}$  can be produced behind a roughly spherical hydrodynamical shock driven by the initial quasi-isotropic expansion of the magnetosphere. The expansion becomes collimated and the tower formation begins only after the stress of the magnetosphere becomes sufficient to balance the post-shock pressure. The collimation process of the magnetar wind thus involves both a quick isotropic expansion followed by a beamed component. We feel that this modification to the magnetar scenario, i.e., the inclusion of the magnetosphere interaction with the exterior star, strengthens its viability as a model for the long GRB central engine.

#### 4.2. Restarting the Engine

We note that the same magnetar can power explosions with the degree of collimation that depends on the magnitude of the outer bounding pressure. A quasi-spherical supernova or a highly beamed jet may result from the same star at different times as the bounding pressure changes. In the collapse and explosion of a massive star, the pressure of stellar gas bounding the central magnetar may have a complex time history. The star may initially collimate the embedded magnetar power into a tightly collimated tower responsible for GRB emission. Subsequently, after the star expands and the pressure bounding the magnetar decreases, the magnetar power will no longer be strongly beamed and a normal quasi-spherical magnetar outflow will result. Later, however, if material not ejected to infinity falls back and accretes, the magnetar will again be surrounded by a bounding pressure and its power will be recollimated. X-ray flares observed following some GRBs (Burrows et al. 2005; Falcone et al. 2006; Romano et al. 2006) could result from this process (see also, e.g., Proga & Zhang 2006; Perna, Armitage & Zhang 2006).

#### 4.3. Pre-shaping the cavity

In the previous sections, we have shown that toroidal field makes the expanding plasma self-collimating due to hoop stress, and propose a spherical cavity with constant wall properties (i.e. no dependence on polar angle) as the simplest model problem. However, the cavity is expected in many cases to have lower density near the polar axis at fixed radius due to various processes acting as the star collapses. Among these are rotational flattening and the asymmetric stress from an early magnetized wind. First, in order to produce a millisecond magnetar, the progenitor star must have been rapidly rotating. We therefore expect the collapsed core to be strongly modified by rotational effects. In particular the material near the rotation axis experiences no centrifugal barrier inhibiting

its accretion, resulting in a relatively low density in the polar region. A separate effect is that a weaker, non-relativistic MHD jet may have been launched along the axis earlier, during the collapse of the stellar core (LeBlanc & Wilson 1970; Wheeler et al. 2000). In addition, an initial MHD wind from the proto-magnetar may be concentrated to the poles as in Bucciantini et al. (2006). This will push out the cavity in the polar region. The subsequent relativistic wind will then expand into a cavity pre-shaped by the previous MHD wind. At a fixed radius, the pressure and density of the wall will be decreased at the poles relative to the equatorial values. If these effects are extreme, the cavity is significantly weakened in the polar direction, and a model problem consisting of a “magnetar-in-a-tube” is of interest.

#### 4.4. Pulsar Kicks

Note that in our picture, most of the magnetically-extracted rotational energy of the neutron star travels vertically through the two oppositely directed channels. Correspondingly, a significant amount of linear momentum is transported up and down from the neutron star and, correspondingly, a back-reaction force is exerted on the neutron star from both the top and the bottom. The two back-reaction forces are oppositely-directed and nearly cancel each other. However, even a slight imbalance in the force may have important consequences for the overall momentum impacted to the neutron star and hence for its terminal velocity. For example, taking the total initial rotational energy of the PNS to be  $E_{\text{rot}} = 5 \cdot 10^{52}$  erg, the momentum transported out in each direction is  $P = E_{\text{rot}}/2c \sim 10^{42}$  cgs. Therefore, just a 10% imbalance would result in the terminal velocity of the neutron star of order of  $v_{\text{term}} \simeq 0.1P/M_{\text{NS}} \sim 300$  km/sec.

#### 4.5. Prospects for Numerical Simulations

In order to gain a solid physical understanding of the fundamental physical processes controlling the interaction of a magnetar with its birth environment, we suggest a sequence of numerical investigations employing a range of well-tested plasma descriptions. Of particular usefulness are limiting cases which allow for simplified analysis making the key physics more transparent. Simulations should cover regions of parameter space where limiting cases overlap with more complete plasma descriptions. For example, force-free (degenerate) electrodynamics (FFDE) is a useful tool for studying highly magnetized plasma for which pressure and inertia are negligibly small. In this extreme case, the cavity wall would have to be represented by a rigid perfectly conducting outer boundary condition. While this case may not be of general relevance for the realistic physical environment, some basic aspects of a bounded rotating magnetosphere may be understood using this description. In addition, the FFDE description has the advantage of requiring fewer parameters to specify the initial and boundary conditions for a given model problem. The results of the time integration can then be more easily understood with a minimum of complicating factors. Time-dependent force-free codes have already been used successfully in the recent years to study pulsar magnetospheres (e.g., Komissarov 2006; McKinney 2006b; Spitkovsky 2006).

It is possible that the full magnetar-in-a-star problem can be successfully investigated by a hybrid simulation that would employ a relativistic force-free code inside the cavity and a relativistic hydrodynamic simulation outside (e.g., R. D. Blandford 2005, private communication, McKinney 2006a).

The next step would be to treat the plasma in the fully relativistic MHD regime. There are several relativistic MHD codes in existence that have reached the required level of maturity (Koide, Shibata & Kudoh 1999; Gammie, McKinney & Tóth 2003; Del Zanna, Bucciantini & Londrillo 2003; De Villiers, Hawley & Krolik 2003; Fragile 2005; Komissarov 2005; Nishikawa et al. 2005). Of interest would be a set of simulations with a range of plasma  $\beta$ . The low- $\beta$  simulations should match on to the FFDE case, at least qualitatively. Once these simulations are analyzed and the basic physical processes elucidated,  $\beta$  can be gradually increased enabling an understanding of how plasma inertia and pressure affect the dynamics of the magnetosphere expansion and collimation.

The basic process of tower formation and collimation can initially be explored with two-dimensional axisymmetric simulations. However, to investigate tower stability to non-axisymmetric disruptions, fully three-dimensional simulations are necessary.

Finally, note that the general processes we describe here are of interest for many astrophysical systems including non-relativistic central objects (e.g., proto-planetary nebulae). For this reason, non-relativistic MHD simulations of this problem are of interest in themselves, as well as a first step toward fully relativistic MHD. Recent non-relativistic MHD simulations indicate that the magnetic tower mechanism can operate successfully in a variety of astrophysical environments (e.g., Romanova et al. 2004; Kato et al. 2004; Nakamura et al. 2006).

## 5. CONCLUSIONS

In this paper we have investigated the millisecond-magnetar scenario for the central engine of Gamma-Ray Bursts and core-collapse Supernovae. We have focused on the interaction between the rapidly-rotating magnetar magnetosphere and the surrounding infalling stellar envelope. We have argued that the stellar material provides a confining (ram) pressure that has a strong effect on both the size and the shape of the magnetosphere. In particular, it can channel the highly-magnetized outflow originating from the proto-neutron star into two collimated magnetic towers.

More specifically, we suggest that the stalled bounce shock — a common feature in models of core-collapse supernovae — effectively plays a role of a cavity that confines the magnetosphere. The cavity's radius, determined by the balance between the pressure of the hot neutrino-heated gas and the ram pressure of the infalling material, stays quasi-stationary at  $R_0 \simeq 200$  km during the first few hundreds of milliseconds after the bounce. To get a feeling for what happens to the magnetar magnetosphere during this stage, we introduce a simplified fundamental-physics problem that we call the *Pulsar-in-a-Cavity* problem. A large part of our paper (§ 2) is devoted to investigating this problem. We show that since the radius of the cavity is larger than the pulsar light-cylinder radius, the magnetic field inside the cavity continuously winds up. Correspondingly, both the toroidal field strength and the magnetic spin-down luminosity of the pulsar increase roughly linearly with time. The magnetic energy in the cavity then grows quadratically with time. We then demonstrate that in the context of a millisecond magnetar inside a collapsing star the magnetic field becomes dynamically important a fraction of a second after the bounce. This leads to a subsequent revival of the stalled shock and may result in a successful magnetically-driven explosion. As long as the expansion of the cavity is non-relativistic, the toroidal mag-

netic field inside it remains larger than the poloidal magnetic and electric fields. As a result, the hoop-stress collimates the Poynting-flux-dominated outflow into two vertical channels that are similar to Lynden-Bell's (1996) magnetic towers (see Uzdensky & MacFadyen 2006).

Finally, we discuss the implications of model for several observationally-motivated questions relevant to GRBs and core-collapse supernovae, such as  $^{56}\text{Ni}$  production, late-time X-ray flares, and pulsar kicks. We also outline a set of numerical studies that we feel need to be done.

AIM acknowledges support from the Keck Fellowship at the Institute for Advanced Study. DAU's research has been supported by the National Science Foundation under Grant PHY-0215581 (PFC: Center for Magnetic Self-Organization in Laboratory and Astrophysical Plasmas).

## REFERENCES

Akiyama, Wheeler, Meier, & Lichtenstadt 2003, ApJ, 584, 954  
 Aloy, M. A., Müller, E., Ibáñez, J. M., Martí, J. M. & MacFadyen, A., 2000, ApJ, 531, 119  
 Arons, J. 2003, ApJ, 589, 871  
 Bethe, H. A., & Wilson, J. R. 1985, ApJ, 295, 14  
 Bethe, H. A. 1990, Rev. Mod. Phys., 62, 801  
 Blandford, R. D., & Znajek, R. L. 1977, MNRAS, 179, 433  
 Bucciantini, N., Thompson, T. A., Arons, J., Quataert, E., & Del Zanna, L. 2006, MNRAS, 368, 1717  
 Burrows, D. N. et al. 2005, Science, 309, 1833  
 Contopoulos, I., Kazanas, D., & Fendt, C. 1999, ApJ 511, 351  
 Della Valle, M., et al. 2006, submitted to Nature; preprint (astro-ph/0608322)  
 Del Zanna, L., Bucciantini, N., & Londrillo, P. 2003, A&A, 400, 397  
 De Villiers, J.-P., Hawley, J. F., & Krolik, J. H. 2003, ApJ, 599, 1238  
 Duncan, R. C., & Thompson, C. 1992, ApJ, 392, L9  
 Falcone, A. D. et al. 2006, ApJ, 641, 1010  
 Fragile, P. C. 2005; preprint (astro-ph/0503305)  
 Fynbo, J. P. U. et al. 2006, submitted to Nature; preprint (astro-ph/0608313)  
 Gal-Yam, A. et al. 2006; preprint (astro-ph/0608257)  
 Gammie, C. F., McKinney, J. C., & Tóth, G. 2003, ApJ, 589, 444  
 Goldreich, P. & Julian, W. H. 1969, ApJ, 157, 869  
 Goldreich, P., Pacini, F., & Rees, M. J. 1971, Comments on Astrophysics and Space Physics, 3, 185  
 Kaneko, Y. et al. 2006, ApJ in press; preprint (astro-ph/0607110)  
 Kardashev, N. S. 1970, Sov. Astron., 14, 375  
 Kato, Y., Hayashi, M. R., & Matsumoto, R. 2004, ApJ, 605, 307  
 Koide, S., Shibata, K., & Kudoh, T. 1999, ApJ, 522, 727  
 Komissarov, S. S. 2005, MNRAS, 359, 801  
 Komissarov, S. 2006, MNRAS, 367, 19  
 LeBlanc, J. M. & Wilson, J. R. 1970, ApJ, 161, 541  
 Lynden-Bell, D. 1996, MNRAS, 279, 389  
 Lyutikov, M. & Blandford, R. 2002, Proceeding of the Workshop on *Beaming and Jets in Gamma Ray Bursts (NBSI)*, ed. R. Ouyed, Copenhagen, Aug. 2002; preprint (astro-ph/0210671)  
 Lyutikov, M. & Blandford, R. 2003; preprint (astro-ph/0312347)

Lyutikov, M. 2006, *New Journal of Physics*, in press; preprint (astro-ph/0512342)

MacFadyen, A. I. & Woosley, S. E. 1999, *ApJ*, 524, 262

MacFadyen, A. I., Woosley, S. E., & Heger, A. 2001, *ApJ*, 550, 410

MacFadyen, A. I. 2003, "Gamma-ray Burst and Afterflow Astronomy: 2001" *AIP Conference Proceedings*, 662, 202

McKinney, J. C. 2006a, *MNRAS*, 367, 1797

McKinney, J. C. 2006b, *MNRAS*, 368, L30

Michel, F. C. 1973, *ApJ*, 180, L133

Nakamura, T. 1998, *Progress of Theoretical Physics*, 100, 921

Nakamura, M., Li, H., & Li, S. 2006, accepted to *ApJ*; preprint (astro-ph/0608326)

Nishikawa, K.-I., Richardson, G., Koide, S., Shibata, K., Kudoh, T., Hardee, P., & Fishman, G. J. 2005, *ApJ*, 625, 60

Ostriker, J. P. & Gunn, J. E. 1971, *ApJ*, 164, L95

Paczynski, B. 1998, *ApJ*, 494, L45

Perna, R., Armitage, P. & Zhang B., 2006, *ApJ* 636, L29

Proga, D. & Zhang, B., 2006, *MNRAS*, 370, 61

Ramirez-Ruiz, E. & Socrates, A. 2005; preprint (astro-ph/0504257)

Romanov, P. et al., 2006, *A&A*, 450, 59

Romanova, M. M., Ustyugova, G. V., Koldoba, A. V., & Lovelace, R. V. E. 2004, *ApJ*, 616, L151

Ruderman, M. A., Tao, L., & Kluzniak, W. 2000, *ApJ*, 542, 243

Soderberg, A., 2006, "Gamma-Ray Bursts in the Swift Era, Sixteenth Maryland Astrophysics Conference" Eds. Holt, S.S., Gehrels, N. & Nousek, J. A., *AIP Conference Proceedings*, 838, 380.

Spitkovsky, A. 2006, *ApJ*, 648, L51

Spruit, H. 1999, *A&A*, 341, L1

Thompson, C. & Duncan, R. C. 1993, *ApJ*, 408, 194

Thompson, C. 1994, *MNRAS*, 270, 480

Thompson, T. A., Chang, P., & Quataert, E. 2004, *ApJ*, 611, 380

Usov, V. V. 1992, *Nature*, 357, 472

Uzdensky, D. A. & MacFadyen, A. I. 2006, *ApJ*, 647, 1192

Wheeler, J. C., Yi, I., Höflich, P., & Wang, L. 2000, *ApJ*, 537, 810

Wheeler, J. C., Meier, D. L., & Wilson, J. R. 2002, *ApJ*, 568, 807

Woosley, S. E. & Weaver, T. A. 1986, *ARA&A*, 24, 205

Woosley, S. E. 1993, *ApJ*, 405, 273

Yi, I. & Blackman, E. G. 1998, *ApJ*, 494, L163

Zhang, W., Woosley, S. E., & MacFadyen, A. I. 2003, *ApJ*, 586, 356